Vortex induced vibrations of marine risers: validating turbulence models

C. Wang, A.E.P. Veldman, E.J. Stamhuis, and A.I. Vakis

***Abstract*—This paper presents results from numerical simulations and laboratory experiments investigating the flow around a circular cylinder at Reynolds numbers (Re) 500 and 3900. Direct numerical simulation (DNS), Reynolds averaged Navier-Stokes (RANS) and large eddy simulation (LES) results are compared for unsteady turbulent flows. For purposes of validation, force measurements conducted in a flow tank are also reported. At $Re = 500$, DNS and LES are used to evaluate the performance of the meshing strategy and the accuracy of the models in 2D cases. At $Re = 3900$, the RANS model is also applied for 2D and compared to DNS and LES. Though the results from the two turbulence models are close to each other, they cannot properly model the physical behavior of the system in 2D. Thus, a 3D case with LES is simulated to investigate the conditions necessary for turbulence modeling to capture the physics of the flow around a cylinder for increasing Re.**

***Index Terms*—Vortex shedding, Circular cylinder flow, CFD, Turbulence modelling, Experiments**

I. Introduction

In ocean engineering, marine risers play an important role, for example, as mooring lines or as cables connecting point absorber wave energy converters to the seabed [1]. Most marine risers are usually cylindrical structures under excitation from currents and waves, with the latter influencing their behavior closer to the water surface. Thus, the problem can be seen as flow around cylinders, which is a key problem in fluid dynamics. Over a wide range of Reynolds numbers (Re), when flow develops around the risers, alternating vortices form at their after-body and shed into the downstream wake with a coherent and periodicity-varied flow pattern of vortices [2]. When the frequency of vortex shedding is equal to or close to the natural frequency of the structure, vortex shedding will cause structural vibrations [3]. As vortex-induced vibrations (VIV) are generated by flows and currents in the subsea, such oscillations can last for a long period of time at high frequencies and produce significant damage that accumulates in structural components. The accumulated damage may eventually lead to the failure of the structure. Furthermore, due to their theoretical significance and rich physics, VIV have attracted more and more attention in the field of fluid-structure interaction in the last few decades.

Computational Fluid Dynamics (CFD) is a very effective and promising way to research the issue of VIV. There are three main approaches adopted in CFD models: direct numerical simulation (DNS), Reynolds-averaged Navier-Stokes (RANS) and Large eddy simulation (LES). The DNS method can be used to solve the flow field in the space and time domains with high precision. However, it consumes a lot of computational resources. At present, this method has been widely used in the numerical simulation of the flow around a fixed cylinder and the eddy-induced vibrations of a rigid cylinder. Despite the DNS method being very accurate, the computational cost increases with increasing Re. As a result, most research with numerical simulations focuses on low Reynolds numbers [4]–[6]. Furthermore, 2D simulations may become inadequate as the underlying physics of the problem change, but a tenfold increase in Re corresponds to 1000 times more computational cost in 3D simulations. This makes it virtually impossible to solve engineering application problems with DNS. In order to efficiently simulate VIV in turbulent flows, turbulence modeling is necessary and constitutes one of the most important aspects of CFD modeling.

In this study, flow around a fixed circular cylinder at $Re = 500$ and $Re = 3900$ is investigated. The former is used as a benchmarking study, while flow at $Re = 3900$, which falls within the lower subcritical range where it remains laminar beyond separation and transition takes place in the free shear layer in the wake, is of greater interest for engineering applications. In this flow regime, the transition waves appear along the free shear layer and the turbulent eddies are shed periodically along the wake of the cylinder. This value of Re has often been investigated in previous studies concerning flows past fixed cylinders as a typical case of the early turbulent regime. By investigating the $Re = 3900$ case with DNS, RANS and LES, we can ensure the validity of our turbulence models when comparing our results with literature. In the following sections, we show that a suitably selected turbulence model is able to capture most of the real physics of the phenomena, including the Kármán vortex street effects on the lift and drag coefficients. A series of

Sponsor and financial support acknowledgement. This study was supported by a fellowship from the China Scholarship Council.

C.Wang is with Computational Mechanical and Materials Engineering, University of Groningen, 9747AG, the Netherlands (e-mail: c.wang@rug.nl).

A.E.P. Veldman is with Computational and Numerical Mathematics, University of Groningen, 9747AG, Groingen and National Aerospace Laboratory, 1006BM, Amsterdam, the Netherlands (e-mail: a.e.p.veldman@rug.nl).

E.J. Stamhuis is with Marine Zoology Biomimetics, University of Groningen, 9747AG, the Netherlands (e-mail: e.j.stamhuis@rug.nl).

A.I. Vakis is with Computational Mechanical and Materials Engineering, University of Groningen, 9747AG, the Netherlands (e-mail: a.vakis@rug.nl).

Digital Object Identifier:
https://doi.org/10.36688/ewtec-2023-342

experimental measurements used to validate the simulations are also reported and the time averaged drag coefficients from numerical simulations are compared to the literature.

II. Numerical method

Simulations are performed using the open source CFD toolbox OpenFOAM. In this section, a detailed account of the setup is given, including the computational domain, boundary conditions and meshing strategy.

A. Governing equations

In fluid mechanics, the Navier-Stokes (N-S) equations are a set of partial differential equations which are used for describing the flow of incompressible fluids. Combining the equations of continuity, momentum and energy, the incompressible N-S equations can be written as follows:

$$\nabla \cdot u = 0 \tag{1}$$

$$\rho \frac{Du}{Dt} = -\nabla p + \mu \nabla \cdot \nabla u + \rho F \tag{2}$$

where u is the flow velocity, t is time, ∇ is the divergence, ρ is the density of the fluid, p is the pressure, μ is the dynamic viscosity of the fluid, $\nabla \cdot \nabla$ is the Laplacian operator, and F is the external force. On the left hand side of the momentum equation, $\frac{Du}{Dt}$ is the total derivative, which includes the convective term. The gradient of p, is a vector representing the change in pressure. In most situations, F is the gravitational force. The continuity equation expresses the conservation of mass.

B. RANS and LES

RANS models solve the Reynolds equation for mean flow quantities only. As a two-equation model, the computational expense of RANS is reduced compared to DNS. RANS is widely used for practical engineering calculations. The key point to closing the RANS equations appropriately is the modeling of the Reynolds stress $-\rho\overline{u_i u_j}$. The standard $k-\omega$ model is well suited for simulating the flow in the sub-viscous layer while the $k-\epsilon$ model is ideal for predicting the flow slightly away from the wall. Further on, the standard $k-\omega$ is more suitable for low-Reynolds number flows, is highly nonlinear, often sensitive to the initial guess and thus more difficult to converge. The $k-\omega$ Shear Stress Transport (SST) turbulence model was originally proposed by Menter [7] as a two-equation eddy-viscosity model. It is a hybrid model that combines the advantages of the $k-\omega$ and $k-\epsilon$ models by switching between them. The $k-\omega$ SST model uses the $k-\omega$ model near the wall and switches to the $k-\epsilon$ model as it approaches the free-stream.

LES, which does not adopt the conventional time- or ensemble-averaging RANS approach with additional modeled transport equations, was proposed by Smagorinsky. It is capable of solving three-dimensional (3D) and transient turbulent flow problems. Only the influence of the small eddies has to be modeled by a subgrid-scale (SGS) model in LES, whereas the large energy-carrying eddies are computed directly. Since most of the turbulent energy is contained in large eddies, LES is more accurate than the RANS approaches and captures these eddies in full detail. Furthermore, the small scales tend to be more isotropic and homogeneous than the large ones, and thus modeling the SGS motions is easier than modeling all scales within a single model as in the RANS approach. In order to separate the large and small scale motions, the three-dimensional, time dependent Navier–Stokes equations are filtered. Currently LES seems to be the most viable numerical tool for simulating realistic turbulent flows.

C. Computational setup

Flow around a circular cylinder in cross flow was taken as a test case at both Reynolds numbers of 500 and 3900. The cross section of the computational domain and the coordinate system are shown in Figure 1. The diameter of the cylinder D is 1 m. The height and width are $20D$ and $40D$ respectively. For three-dimensional modeling, the computation domain has extents of πD in the spanwise direction.

The inlet velocity is fixed at 1 m/s. The outlet is just downstream of the cylinder, and the outlet pressure is set to zero. When a fluid flows through a solid surface, it will come to a complete stop at the surface and the velocity relative to the surface (both normal and tangential) is assumed to be zero. Therefore, the cylinder is set to 'no-slip' condition where pressure is set to zero gradient and velocities are set to zero. The top and bottom boundaries are set to 'slip' condition. The front and back of the cylinder are defined as side walls. In 2D problems, side walls are defined in a single patch with type 'empty'. For 3D problems, the flow is assumed to be periodic in the spanwise direction.

Pressure-velocity coupling is solved via the Pressure Implicit with Split Operators (PISO) method. The implicit second-order Crank-Nicolson scheme is used for the time integration. The divergence and gradient terms are discretized using the Gauss linear integration scheme. The Laplacian and surface normal gradients are discretized using Gauss linear integration with

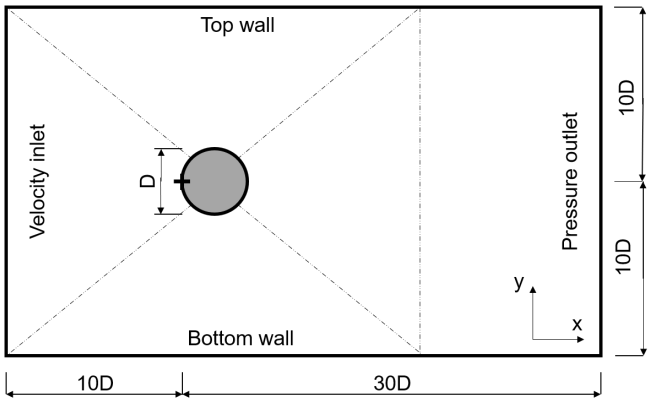

Fig. 1. Schematic presentation of the computational domain

limited non-orthogonal correction. All the employed schemes are formally of second-order accuracy.

The inputs for the inlet velocity for different Reynolds Numbers are calculated using the following formula

$$Re = \frac{\rho u D}{\mu}, \tag{3}$$

where u is the inlet velocity and D is the characteristic length, which equals the diameter of the circular cylinder in this case.

Hexahedral grids are generated by the O-type grid in the computational domain. The domain is divided into 5 blocks, delineated by dotted lines in Figure 1. The grids are clustered near the cylinder and the spacing is increased in fixed ratios. Figure 2 shows an example of the meshing design around the cylinder. At $Re = 500$, 2D simulations are taken with coarse to fine grids to run a convergence study for the DNS and LES models. At $Re = 3900$, with the same meshing strategies, different turbulence models are taken into account.

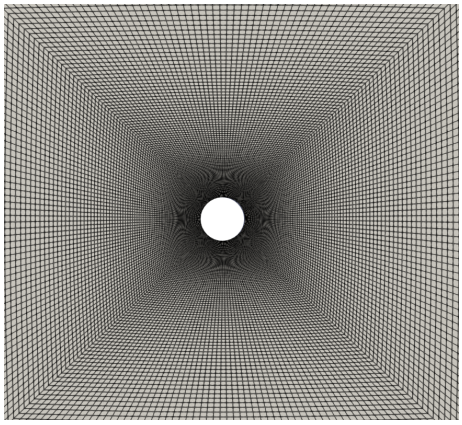

Fig. 2. Schematic of computational grids around the cylinder

III. Results and discussion

Flow past a circular cylinder is simulated to verify the relative advantage of the hybrid turbulence models RANS and LES compared to DNS. The time averaged drag coefficient (C_d^m), root mean square value lift coefficient (C_l^r) and Strouhal number (St) are calculated to evaluate the results of different cases. The Strouhal number is defined as $St = fD/U$, where f is the frequency of the lift force, D is the diameter of the cylinder, and U is the mean inlet velocity at the cylinder location. During post-processing, St is computed from the lift coefficient (C_l) time histories. To get reliable and more accurate results, the time step and grid size are adjusted to make the maximum Courant–Friedrichs–Lewy (CFL) number lower than 2. The CFL condition expresses that the distance that any information travels during the time step length within the mesh must be lower than the distance between mesh elements. According to the CFL number, the time step has to be assigned for each case. The total calculation time is 500 seconds for all cases.

TABLE I
Convergence studies at $Re = 500$ with DNS

Case	Grid	Δt (s)	C_d^m	C_l^r	St
*c*ase1	8,370	0.020	1.518	0.857	0.217
*c*ase2	32,635	0.020	1.498	0.888	0.223
*c*ase3	128,865	0.007	1.473	0.865	0.227
*c*ase4	288,695	0.005	1.460	0.850	0.226
*c*ase5	512,125	0.003	1.460	0.853	0.226
*R*ef [8]	-	-	1.448-1.461	-	0.228
*R*ef [9]	-	-	1.463	-	0.23

TABLE II
Convergence studies at $Re = 500$ with LES

Case	Grid	Δt (s)	C_d^m	C_l^r	St
*c*ase2	32,635	0.020	1.501	0.880	0.223
*c*ase3	128,865	0.007	1.474	0.857	0.226
*c*ase4	288,695	0.005	1.465	0.851	0.227
*c*ase5	512,125	0.003	1.462	0.849	0.227

A. Re=500

For $Re = 500$, the case with the coarsest grid contains 8,370 elements, while the finest grid case has 512,125 elements. The grid size in the spanwise direction is set to 1, so that the LES model can also be used for these 2D calculations.

The strategy to study convergence was to first run the simulation at a very coarse grid level. The global parameters of the flow are compared in Table I and Table II. After a series of grid refinement studies, the force coefficient and St are converged. The results of two models are very close and agree with each other in 2 decimals. The C_d^m values from the finest grid are in line with previous studies reported in the literature [8], [9]. The convergence of the Strouhal numbers from coarser to finer grids is more continuous and occurs faster than that of the force coefficients. The converged results are in good agreement with the published data [10].

B. Re=3900

Maintaining the same meshing design, simulations at $Re = 3900$ are first ran in 2D. For the grid refinement study, four cases with coarse to fine grids are applied. The C_d^m, C_l^r and St from different turbulence models are summarized in Tables III to V. Most results are converged to one decimal. The C_d^m and St from the $k-\omega$ SST model are more stable than those for the other two models; however, the results are not in agreement with published experimental data.

Flows with Re between 300 to 2×10^5 are in the so-called sub-critical range, for which 2D simulations are no longer reliable, even though the results from the different turbulence models are close to each other. Hence, a 3D simulation with LES is also performed for $Re = 3900$. The same 2D mesh was copied to 16 spanwise intervals and a volume mesh was created yielding 522,160 cells. The drag and lift forces varied with time shown in Figure 4. In this case, we get C_d^m is

TABLE III
CONVERGENCE STUDIES AT Re=3900 WITH 2D DNS

Case	Grid	Δt (s)	C_d^m	C_l^r	St
case1	32,635	0.020	1.776	0.690	0.215
case2	72,800	0.010	1.765	0.698	0.203
case3	128,865	0.007	1.677	0.706	0.234
case4	288,695	0.005	1.586	0.691	0.247

TABLE IV
CONVERGENCE STUDIES AT Re=3900 WITH 2D $k-\omega$ SST

Case	Grid	Δt (s)	C_d^m	C_l^r	St
case1	32,635	0.020	1.711	0.607	0.245
case2	72,800	0.010	1.705	1.196	0.243
case3	128,865	0.007	1.685	1.188	0.243
case4	288,695	0.005	1.677	1.179	0.247

TABLE V
CONVERGENCE STUDIES AT Re=3900 WITH 2D LES

Case	Grid	Δt (s)	C_d^m	C_l^r	St
case1	32,635	0.020	1.684	0.638	0.234
case2	72,800	0.010	1.721	0.692	0.227
case3	128,865	0.007	1.779	0.709	0.241
case4	288,695	0.005	1.758	0.694	0.263

0.982 which in good agreement with existing numerical and experimental studies. At the same time, St is 0.243, which is outside the range reported based on experimental data. Compared to the studies performed in the literature, summarized in Figure 3, much finer grids are required to get more accurate results.

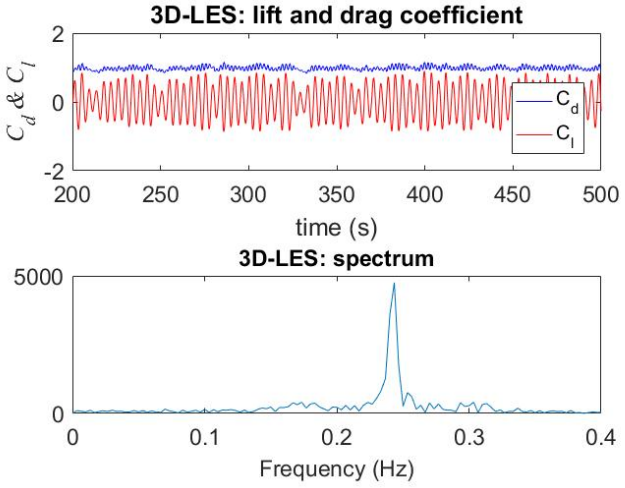

Fig. 3. Time history of drag and lift coefficients for 3D LES model ($Re = 3900$)

C. Experimental investigations

Measurements are performed in a circulating flow tank with a 0.40 m× 0.40 m × 2.0 m test section. The cylinder is made of acrylic with a diameter of 20 mm and a length of 350 mm. Both sides of the cylinder are

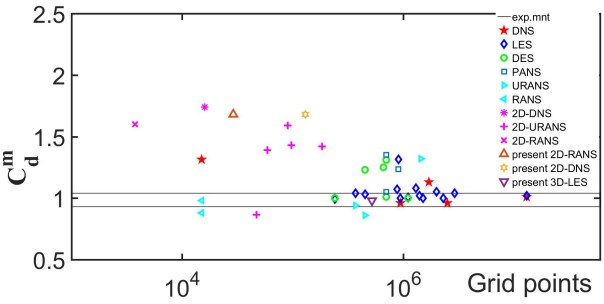

Fig. 4. C_d^m comparisons between literature survey and present work. Experimental values are obtained from [11], [12], DNS values are obtained from [13]–[16], LES results are obtained from [16]–[29], RANS results are obtained from [23], [30], DES results are obtained from [21], [30]–[33], PANS results are obtained from [31], [34], URANS results are obtained from [21], [29], [35]–[37].

fixed and connected to the frame, as shown in Figure 4. The whole frame is immersed in the water.

On the top, a metal rod of diameter 5 mm is used to connect the force sensor to the cylinder frame. With the force sensor (10 N measuring range), both the lift and drag forces can be measured. To get the forces of the cylinder, firstly, the force measurements of the whole frame are conducted. Then, the cylinder is removed and the force on the bracket is measured for the same flow conditions such that the response of the cylinder alone can be isolated. The flow tank is equipped with a variable speed pump, which can induce velocities varying from 0.05 m/s to 0.3 m/s, corresponding to Re from 1000 to 7000. The circulation channel water temperature, measured during the experiments, was 21.5 ± 0.5 °C.

At $Re = 3900$, the drag coefficient measured in the experiments is 1.01, which is in the range of what has been reported in the literature and agrees with the reported numerical results.

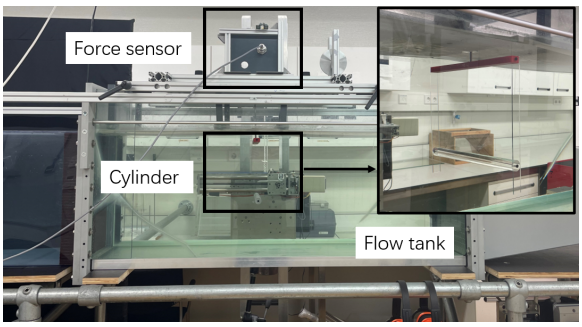

Fig. 5. Experimental setup for force measurements

IV. CONCLUSIONS

Simulations of a cylinder in cross flow performed at $Re = 500$ with two-dimensional DNS and LES are shown to converge and match the values reported in the literature, which verifies the choice of space and time discretization. The converged mesh is then adopted two-dimensional DNS, RANS and LES simulations at $Re = 3900$. Furthermore, experiments were performed at $Re = 3900$ yielding a time averaged drag coefficient of 1.01, which is in the range of 0.94–1.04

reported in the literature [6]. While most results across the various methods are converged, two-dimensional simulations yield incorrect results. Therefore, an LES simulation was performed in 3D, which yields a drag coefficient of 0.982 that agrees well with the experiments and literature [38], even though the Strouhal number of 0.243 is still outside the expected range. This suggests that 3D LES with even finer discretization is necessary to properly capture the physics of the flow in the sub-critical range.

ACKNOWLEDGEMENT

This study was supported by a fellowship from the China Scholarship Council. We thank the Center for Information Technology of the University of Groningen for their support and for providing access to the Hábrók high performance computing cluster.

REFERENCES

[1] W. He, X. He, and S. S. Ge, "Vibration control of flexible marine riser systems with input saturation," *IEEE/ASME Transactions on Mechatronics*, vol. 21, no. 1, pp. 254–265, 2015.

[2] J.-s. Wang, D. Fan, and K. Lin, "A review on flow-induced vibration of offshore circular cylinders," *Journal of Hydrodynamics*, vol. 32, no. 3, pp. 415–440, 2020.

[3] N. B. Khan, Z. Ibrahim, M. I. Khan, T. Hayat, and M. F. Javed, "Viv study of an elastically mounted cylinder having low mass-damping ratio using rans model," *International Journal of Heat and Mass Transfer*, vol. 121, pp. 309–314, 2018.

[4] S. Singh and S. Mittal, "Vortex-induced oscillations at low reynolds numbers: hysteresis and vortex-shedding modes," *Journal of fluids and structures*, vol. 20, no. 8, pp. 1085–1104, 2005.

[5] T. Prasanth and S. Mittal, "Vortex-induced vibrations of a circular cylinder at low reynolds numbers," *Journal of Fluid Mechanics*, vol. 594, pp. 463–491, 2008.

[6] S. Wornom, H. Ouvrard, M. V. Salvetti, B. Koobus, and A. Dervieux, "Variational multiscale large-eddy simulations of the flow past a circular cylinder: Reynolds number effects," *Computers & Fluids*, vol. 47, no. 1, pp. 44–50, 2011.

[7] F. R. Menter, "Two-equation eddy-viscosity turbulence models for engineering applications," *AIAA journal*, vol. 32, no. 8, pp. 1598–1605, 1994.

[8] H. M. Blackburn and R. D. Henderson, "A study of two-dimensional flow past an oscillating cylinder," *Journal of Fluid Mechanics*, vol. 385, pp. 255–286, 1999.

[9] M. Zhao, L. Cheng, B. Teng, and D. Liang, "Numerical simulation of viscous flow past two circular cylinders of different diameters," *Applied Ocean Research*, vol. 27, no. 1, pp. 39–55, 2005.

[10] Y.-G. Liu and L.-H. Feng, "Suppression of lift fluctuations on a circular cylinder by inducing the symmetric vortex shedding mode," *Journal of Fluids and Structures*, vol. 54, pp. 743–759, 2015.

[11] C. Norberg, "Effects of reynolds number and a low-intensity freestream turbulence on the flow around a circular cylinder," *Chalmers University, Goteborg, Sweden, Technological Publications*, vol. 87, no. 2, pp. 1–55, 1987.

[12] L. Lourenco and C. Shih, "Characteristics of the plane turbulent near wake of a circular cylinder: A particle image velocity study (private communication), reported by kravchenko, ag, moin, p., 2000. numerical studies of flow over a circular cylinder at red= 3900," *Phys. Fluids*, vol. 12, pp. 403–417, 1993.

[13] O. Lehmkuhl, I. Rodríguez, R. Borrell, and A. Oliva, "Low-frequency unsteadiness in the vortex formation region of a circular cylinder," *Physics of Fluids*, vol. 25, no. 8, p. 085109, 2013.

[14] M. T. Dröge, *Cartesian grid methods for turbulent flow simulation in complex geometries*. University Library Groningen][Host], 2006.

[15] X. Ma, G.-S. Karamanos, and G. Karniadakis, "Dynamics and low-dimensionality of a turbulent near wake," *Journal of fluid mechanics*, vol. 410, pp. 29–65, 2000.

[16] P. Beaudan and P. Moin, "Numerical experiments on the flow past a cylinder at sub-critical reynolds number," *Report No. TF*, vol. 62, 1994.

[17] I. Afgan, Y. Kahil, S. Benhamadouche, and P. Sagaut, "Large eddy simulation of the flow around single and two side-by-side cylinders at subcritical reynolds numbers," *Physics of Fluids*, vol. 23, no. 7, p. 075101, 2011.

[18] N. Alkishriwi, M. Meinke, and W. Schröder, "A large-eddy simulation method for low mach number flows using preconditioning and multigrid," *Computers & fluids*, vol. 35, no. 10, pp. 1126–1136, 2006.

[19] A. G. Kravchenko and P. Moin, "Numerical studies of flow over a circular cylinder at re d= 3900," *Physics of fluids*, vol. 12, no. 2, pp. 403–417, 2000.

[20] J. Franke and W. Frank, "Large eddy simulation of the flow past a circular cylinder at red= 3900," *Journal of wind engineering and industrial aerodynamics*, vol. 90, no. 10, pp. 1191–1206, 2002.

[21] X. Han and S. Krajnović, "Validation of a novel very large eddy simulation method for simulation of turbulent separated flow," *International Journal for Numerical Methods in Fluids*, vol. 73, no. 5, pp. 436–461, 2013.

[22] S. Jee, J. Joo, and G. Medic, "Large-eddy simulation of a high-pressure turbine vane with inlet turbulence," in *Turbo Expo: Power for Land, Sea, and Air*, vol. 49729. American Society of Mechanical Engineers, 2016, p. V02DT44A019.

[23] H. Lübcke, T. Rung, F. Thiele *et al.*, "Comparison of les and rans in bluff-body flows," *Journal of wind engineering and industrial aerodynamics*, vol. 89, no. 14-15, pp. 1471–1485, 2001.

[24] R. Mittal, "Progress on les of flow past a circular cylinder," *Center for Turbulence Research Annual Research Briefs*, pp. 233–241, 1996.

[25] J. Fröhlich, W. Rodi, P. Kessler, S. Parpais, J. Bertoglio, and D. Laurence, "Large eddy simulation of flow around circular cylinders on structured and unstructured grids," *Numerical Flow Simulation I: CNRS-DFG Collaborative Research Programme, Results 1996–1998*, pp. 319–338, 1998.

[26] K. Mahesh, G. Constantinescu, and P. Moin, "A numerical method for large-eddy simulation in complex geometries," *Journal of Computational Physics*, vol. 197, no. 1, pp. 215–240, 2004.

[27] N. Park, J. Y. Yoo, and H. Choi, "Discretization errors in large eddy simulation: on the suitability of centered and upwind-biased compact difference schemes," *Journal of Computational Physics*, vol. 198, no. 2, pp. 580–616, 2004.

[28] M. Breuer, "Large eddy simulation of the subcritical flow past a circular cylinder: numerical and modeling aspects," *International journal for numerical methods in fluids*, vol. 28, no. 9, pp. 1281–1302, 1998.

[29] M. Young and A. Ooi, "Comparative assessment of les and urans for flow over a cylinder at a reynolds number of 3900," 2007.

[30] S. Jee and K. Shariff, "Detached-eddy simulation based on the v2-f model," *International journal of heat and fluid flow*, vol. 46, pp. 84–101, 2014.

[31] D. Luo, C. Yan, H. Liu, and R. Zhao, "Comparative assessment of pans and des for simulation of flow past a circular cylinder," *Journal of Wind Engineering and Industrial Aerodynamics*, vol. 134, pp. 65–77, 2014.

[32] V. D'Alessandro, S. Montelpare, and R. Ricci, "Detached–eddy simulations of the flow over a cylinder at re= 3900 using openfoam," *Computers & Fluids*, vol. 136, pp. 152–169, 2016.

[33] R. Zhao, J. Liu, and C. Yan, "Detailed investigation of detached-eddy simulation for the flow past a circular cylinder at re= 3900," in *Progress in Hybrid RANS-LES Modelling: Papers Contributed to the 4th Symposium on Hybrid RANS-LES Methods, Beijing, China, September 2011*. Springer, 2012, pp. 401–412.

[34] D. Reyes, S. Lakshmipathy, and S. Girimaji, "Partially averaged navier-stokes method: Modeling and simulation of low reynolds number effects in flow past a circular cylinder," in *6th AIAA Theoretical Fluid Mechanics Conference*, p. 3107.

[35] T. Ayyappan and S. Vengadesan, "Influence of staggering angle of a rotating rod on flow past a circular cylinder," *Journal of fluids engineering*, vol. 130, no. 3, 2008.

[36] C. Marongiu, P. Catalano, M. Amato, and G. Iaccarino, "U-zen: a computational tool solving u-rans equations for industrial unsteady applications," in *34th AIAA Fluid Dynamics Conference and Exhibit*, 2004, p. 2345.

[37] Y. M. Shim, R. Sharma, and P. Richards, "Numerical study of the flow over a circular cylinder in the near wake at reynolds number 3900," in *39th AIAA Fluid Dynamics Conference*, 2009, p. 4160.

[38] R. Violette, E. De Langre, and J. Szydlowski, "Computation of vortex-induced vibrations of long structures using a wake oscillator model: comparison with dns and experiments," *Computers & structures*, vol. 85, no. 11-14, pp. 1134–1141, 2007.